Received: 15 October 2021 | Revised: 31 January 2022 | Accepted: 7 February 2022

DOI: 10.1111/mpp.13198

Molecular Plant Pathology WILEY

SHORT COMMUNICATION

HopAZ1, a type III effector of *Pseudomonas amygdali* pv. *tabaci*, induces a hypersensitive response in tobacco wildfire-resistant *Nicotiana tabacum* 'N509'

Sachi Kashihara | **Takafumi Nishimura** | **Yoshiteru Noutoshi** | **Mikihiro Yamamoto** | **Kazuhiro Toyoda** | **Yuki Ichinose** | **Hidenori Matsui**

Graduate School of Environmental and Life Science, Okayama University, Okayama, Japan

Correspondence
Hidenori Matsui, Graduate School of Environmental and Life Science, Okayama University, Okayama, Japan.
Email: hmatsui@okayama-u.ac.jp

Funding information
Japan Society for the Promotion of Science, Grant/Award Number: 19H02956

Abstract

Pseudomonas amygdali pv. *tabaci* (formerly *Pseudomonas syringae* pv. *tabaci*; Pta) is a gram-negative bacterium that causes bacterial wildfire disease in *Nicotiana tabacum*. The pathogen establishes infections by using a type III secretion system to inject type III effector proteins (T3Es) into cells, thereby interfering with the host's immune system. To counteract the effectors, plants have evolved disease-resistance genes and mechanisms to induce strong resistance on effector recognition. By screening a series of Pta T3E-deficient mutants, we have identified HopAZ1 as the T3E that induces disease resistance in *N. tabacum* 'N509'. Inoculation with the Pta Δ*hopAZ1* mutant did not induce resistance to Pta in N509. We also found that the Pta Δ*hopAZ1* mutant did not induce a hypersensitive response and promoted severe disease symptoms in N509. Furthermore, a C-terminal truncated HopAZ1 abolished HopAZ1-dependent cell death in N509. These results indicate that HopAZ1 is the avirulence factor that induces resistance to Pta by N509.

KEYWORDS
effector, hypersensitive responses, *Pseudomonas syringae* pv. *tabaci*, type III secretion system

Plant breeding has successfully introduced disease resistance to pathogenic microorganisms into a wide range of economically important plant species. Plant breeders have found disease resistance in wild or cultivated relatives and, where available, have introduced these genes into crops by backcrossing. *Nicotiana tabacum* (tobacco) has a long production history as a nonfood crop worldwide and is frequently used as a molecular model in studies of plant–microbe interactions. From such studies, tobacco cultivars showing bacterial wildfire resistance (Knoche et al., 1987) have been produced; however, the molecular basis by which these disease-resistant cultivars recognize the pathogen remains unclear.

The molecular processes involved in plant disease resistance are well understood as providing two layers of defence: pathogen-associated molecular pattern (PAMP)-triggered immunity (PTI) and effector-triggered immunity (ETI; Jones & Dangl, 2006). Recent papers have shown that the molecular mechanisms of PTI and ETI are interlinked in a complex manner (Yuan et al., 2021). PTI functions to control opportunistic infections through the recognition of PAMPs

Sachi Kashihara and Takafumi Nishimura contributed equally.

by plant pattern recognition receptors. ETI suppresses pathogen infections by inducing a hypersensitive response (HR) to effectors secreted by the pathogen through direct or indirect recognition of the effectors by the plant resistance (*R*) gene product. Because ETI can induce strong resistance, including an HR, it has been used for molecular breeding focusing on *R* genes (Ayliffe, 2004); however, the pairs of *R* genes and their effectors required to induce ETI in many crop species remain to be identified (Kourelis & van der Hoorn, 2018).

Pseudomonas amygdali pv. *tabaci* (formerly *Pseudomonas syringae* pv. *tabaci*; Pta) causes bacterial wildfire disease on the foliage of host tobacco plants. The Pta virulence factors include tabotoxin, a phytotoxin involved in causing chlorosis, and type III effectors (T3Es) that are secreted via the type III secretion system (T3SS). The T3Es function as virulence factors, contributing to the establishment of infection by inhibiting the immune response of the host plant and by altering the host tissue environment to conditions suitable for pathogen growth (Block & Alfano, 2011; Xin et al., 2018). The number of T3Es in Pta strains is estimated to be about 20, based on genomic analysis of Pta strains 6605 and 11528 (Baltrus et al., 2011; Matsui et al., 2021; Studholme, 2011). The T3SS-deficient mutant of Pta 6605 is nonpathogenic. Some T3Es of Pta 11528 suppress reactive oxygen species (ROS) production and defence gene expression after flagellin peptide flg22 treatment, and $HopX1_{Pta11528}$ plays a role in reopening the stomatal pores by affecting jasmonic acid signalling (Gimenez-Ibanez et al., 2014, 2018; Marutani et al., 2005). Thus, Pta is proposed to establish infections by secreting T3Es into the host plant and perturbing the host's immune response.

In most of the studies to date, compatible interactions between Pta and tobacco plants have been investigated. In contrast, there are few studies on the incompatible interaction between Pta and tobacco plants. This study investigated tobacco cultivars showing resistance to the highly virulent Pta strain 6605 and performed experiments to elucidate how Pta-resistant tobacco cultivars recognize Pta 6605.

To confirm resistance to Pta 6605, we conducted a flood inoculation test using nine tobacco lines with different levels of Pta resistance, comprising seven *N. tabacum* cultivars and two other *Nicotiana* species (File S1). Water-soaked lesions were observed 3 days postinoculation (dpi) on *N. tabacum* 'Xanthi', 'BY4', 'Matsukawa', 'Shiroensyu', 'Tsukuba-ichigou' (hereafter Tsukuba), and *Nicotiana benthamiana*, but not *N. tabacum* 'Burley 21', 'N509', or *Nicotiana longiflora* (Figures 1a and S1a,b). *N. benthamiana* is highly susceptible to Pta 6605, and the leaf area was dramatically reduced. For this reason, the water-soaking area could not be measured in *N. benthamiana*. In Burley 21, N509, and *N. longiflora*, no reduction in leaf area was observed after infection with Pta (Figure S1c). We measured the bacterial population of wild-type (WT) Pta 6605 inoculated on these tobacco lines. Consistent with the suppression of disease symptom development, Burley 21, N509, and *N. longiflora* had low bacterial populations of Pta 6605 at 3 dpi. These data suggest that Burley 21, N509, and *N. longiflora* are resistant to Pta 6605 (Figure 1b).

Cultivar N509 was produced by introducing the Pta resistance of cv. Burley 21 into cv. Shiroensyu. Because the Pta resistance in cv. Burley 21 was originally introduced by crossing *N. tabacum* with *N. longiflora* (Heggestad et al., 1960), N509 is hypothesized to have inherited Pta resistance from *N. longiflora*. In our experiments, we used Shiroensyu as the Pta-susceptible cultivar and N509 as the Pta-resistant cultivar. To examine whether Pta resistance in N509 was due to the recognition of a T3E, we checked the HR induction using an infiltration test of the Pta 6605 Δ*hrcC* mutant that lacks a T3SS. As expected, the Pta 6605Δ*hrcC* mutant did not induce an HR (Figure S1).

We hypothesized that N509 recognizes a Pta T3E to induce disease resistance. Accordingly, we generated a series of 18 effector-deficient mutants in the genome of Pta 6605 (Table 1 and Figure S3). To search for Pta 6605 T3Es, we used the genomic data of Pta 6605 from the *Pseudomonas* genome database (Winsor et al., 2016) and the complete genome sequence of Pta 6605 (Matsui et al., 2021). Vector construction and the primers used in our study are described in Figure S3 and Table S1. A homologous recombination approach using pK18*mobsacB* (Schäfer et al., 1994) generated the Pta 6605 T3E deletion mutants. To facilitate the cloning process, we used the multicloning site of pK18*mobsacB* with the addition of a *Not*I site (pK18*mobsacB*N). The *hopM1-avrF*, *hopAG1-hopAH1-hopAI1*, and *hopT1-hopO1* genes are located close to each other on the Pta 6605 chromosome; thus, these mutants were produced as multiple effector-deficient mutants. PCR confirmed each Pta T3E deletion mutant as lacking the target T3E gene(s).

To determine the effect of each Pta 6605 T3E deletion mutant on the disease resistance of N509, we conducted a flood inoculation test. Typically, the leaves of resistant N509 are subject to yellowing following flood inoculation with Pta 6605, but no water-soaked lesions are observed. Interestingly, when the Pta 6605 Δ*hopAZ1* mutant was inoculated on N509, severe disease symptoms similar to those of the susceptible Shiroensyu were observed (Figure 2). This result suggests that the Pta resistance of N509 is possibly associated with the recognition of Pta T3E hopAZ1.

To investigate whether HopAZ1 functions as an avirulence factor against resistance in N509, we produced a complementary strain, Pta 6605 Δ*hopAZ1* carrying p*hopAZ1* (Table 1 and File S1). Inoculation with Pta 6605 and the *hopAZ1* complementation strains resulted in a resistant phenotype for the N509 cultivar (Figure 3a). No difference in the size of bacterial populations for the Shiroensyu cultivar was found between the Pta 6605 Δ*hopAZ1* mutant and complementary strains compared with Pta 6605 (Figure 3b). The Pta 6605 Δ*hopAZ1* mutant had an increased bacterial population compared to the Pta 6605 in N509 (Figure 3c). These results suggest that HopAZ1 is recognized by N509 as an avirulence factor and induces disease resistance against Pta 6605. Next, we examined the ability of HopAZ1 to induce an HR in N509 using a syringe-infiltration method. The Pta 6605 Δ*hopAZ1* strain did not induce an HR in N509, and its ability to induce an HR on N509 was recovered on complementation with *hopAZ1* (Figure 3d). Accordingly, we also confirmed an HR induction in the resistant Burley 21 and in *N. longiflora*. We found

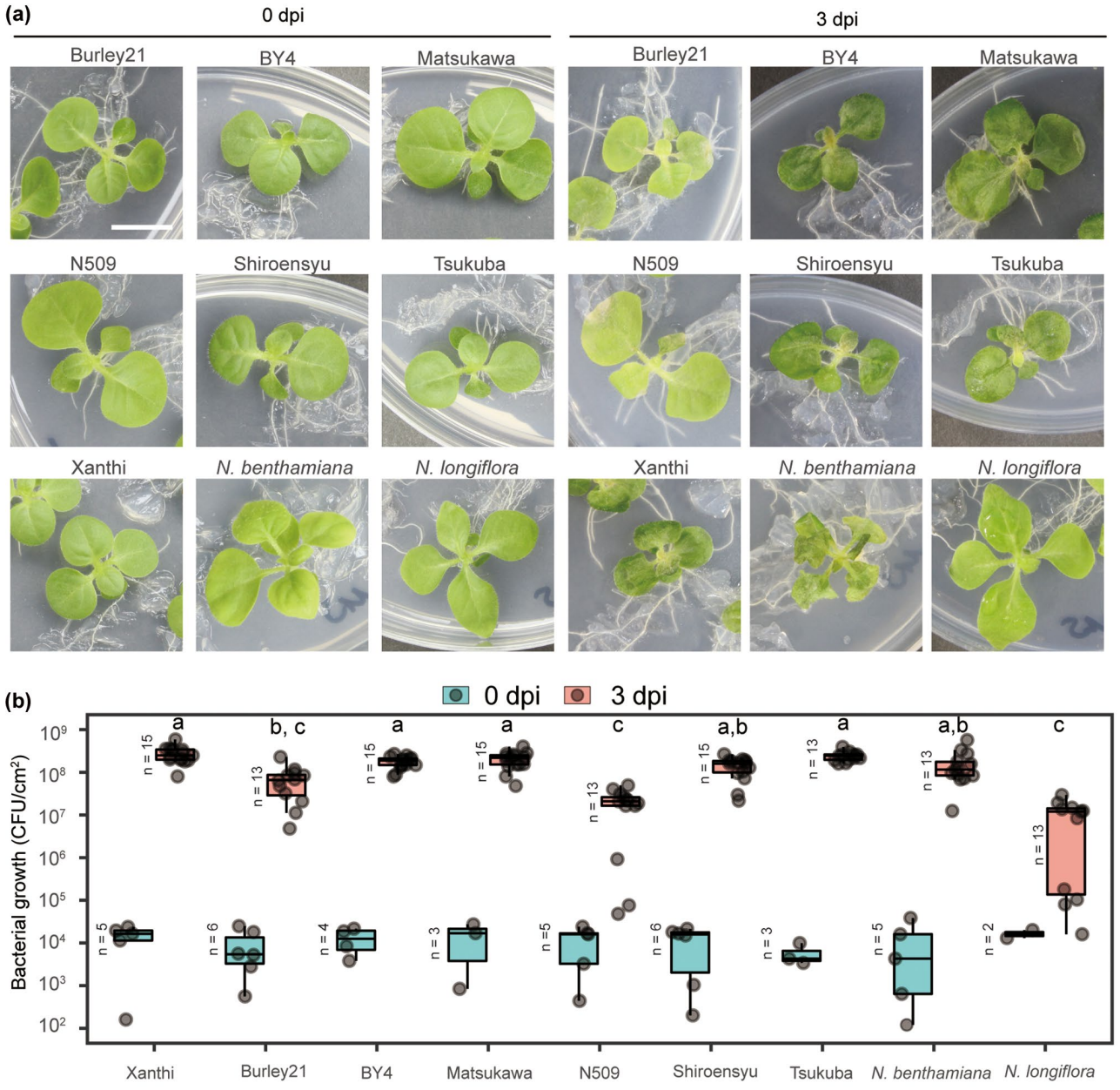

FIGURE 1 *Pseudomonas amygdali* pv. *tabaci* (Pta) 6605 inoculation test in tobacco cultivars and *Nicotiana* species. (a) Photographs of Pta 6605-inoculated tobacco plants. Two-week-old plants of seven *Nicotiana tabacum* cultivars and two other *Nicotiana* species grown on 9-cm Petri dishes were flood-inoculated with a Pta 6605 wild-type (WT) inoculum whose concentration was adjusted to an OD_{600} = 0.02. Plants were photographed 0 and 3 days postinoculation (dpi). The scale bar represents 1 cm. (b) Bacterial population tests on tobacco cultivars and two other *Nicotiana* species. Plants were flood-inoculated with Pta 6605 WT, and bacterial populations were measured at 0 and 3 dpi. The results of two independent experiments were combined and are illustrated in the box plot. Boxes show upper and lower quartiles of the data, and black lines represent the medians. Each dot represents a raw data point. *n* indicates the total number of biological replicates of plants used in the two independent experiments. Statistically significant differences are indicated by different letters ($p < 0.01$, Tukey HSD test)

that the HopAZ1-dependent HR at 24 h postinoculation (hpi) was prominent in Burley 21 but was weak or barely detectable in *N. longiflora* (Figure S4). We also generated a complementary strain with 3 × HA tag added to the C-terminus, but *HopAZ1*-3×HA complementary strains did not induce an HR in N509 and Burley 21 (Figure S5). To quantify the degree of cell death caused by HopAZ1, we measured electrolyte leakage, an indicator of cell death. Consistent with the results of HR induction, electrolyte leakage at 24 hpi was significantly increased in Pta 6605 and Pta 6605 Δ*hopAZ1* (p*hopAZ1*) strains inoculated on N509 (Figure 3e).

The amino acid sequence of HopAZ1 is conserved in several *Pseudomonas* species, but the structure and enzymatic activity of HopAZ1 as an effector has not been determined (Dillon et al., 2019; O'Brien et al., 2012). HopAZ1 of *Pseudomonas savastanoi* pv. *savastanoi*

TABLE 1 Bacterial strains and plasmids

Bacterial strain/plasmid	Relevant characteristics	Reference or source
Escherichia coli		
DH5α	F⁻ λ⁻ *ø80dLacZ ΔM15 Δ(lacZYA-argF)U169 recA1 endA1 hsdR17*($r_K^-m_K^+$) *supE44 thi-1 gyrA relA1*	Takara
S17-1	*thi pro hsdR hsdR hsdM*⁺*recA(chr::RP4-2-Tc::Mu-Km::*Tn*7)*	Schäfer et al. (1994)
Agrobacterium tumefaciens C58C1	pCR32, Tet^R	Holsters et al. (1980)
Pseudomonas syringae pv. *tabaci* (Pta)		
Isolate 6605	Wild type isolated from tobacco, Nal^r	Shimizu et al. (2003)
Pta Δ*hrcC*	Isolate 6605 ΔRS0106115, Nal^r	Marutani et al. (2005)
Pta Δ*avrE1*	Isolate 6605 ΔRS0100760, Nal^r	This study
Pta Δ*avrPto4*	Isolate 6605, Δ*avrPto4*, Nal^r	This study
Pta Δ*hopAB3*	Isolate 6605 ΔRS0105230, Nal^r	This study
Pta Δ*hopAE1*	Isolate 6605 ΔRS0125645, Nal^r	This study
Pta Δ*hopAG1*Δ*hopAH1*Δ*hopAI1*	Isolate 6605 ΔRS0109770, ΔRS0109780, ΔRS0109785, Nal^r	This study
Pta Δ*hopAH2*	Isolate 6605 ΔRS0116920, Nal^r	This study
Pta Δ*hopAR1*	Isolate 6605, Δ*hopAR1*, Nal^r	This study
Pta Δ*hopAS1*	Isolate 6605, ΔRS0114820, Nal^r	This study
Pta Δ*hopAZ1*	Isolate 6605, ΔRS0124775, Nal^r	This study
Pta Δ*hopBD1*	Isolate 6605, Δ*hopBD1*, Nal^r	This study
Pta Δ*hopE1*	Isolate 6605, ΔRS0112920, Nal^r	This study
Pta Δ*hopI1*	Isolate 6605, ΔRS0109130, Nal^r	This study
Pta Δ*hopM1*Δ*avrF*	Isolate 6605, ΔRS0100770, Nal^r	This study
Pta Δ*hopO1-1*Δ*hopT1-1*	Isolate 6605, ΔRS01135, ΔRS01130, Nal^r	This study
Pta Δ*hopR1*	Isolate 6605, Δ*hopR1*, Nal^r	This study
Pta Δ*hopV1*	Isolate 6605, Δ*hopV1*, Nal^r	This study
Pta Δ*hopW1*	Isolate 6605, ΔRS0116415, Nal^r	This study
Pta Δ*hopX1*	Isolate 6605, ΔRS0121235, Nal^r	This study
Pta Δ*hopAZ1*(phopAZ1)	Isolate 6605 ΔRS0124775 carrying pDSK519-*hopAZ1* promoter::*hopAZ1*, Nal^r, Km^r	This study
Pta Δ*hopAZ1*(phopAZ1$^{1\text{-}100}$)	Isolate 6605 ΔRS0124775 carrying pDSK519-*hopAZ1* promoter::*hopAZ1*$^{1\text{-}100}$, Nal^r, Km^r	This study
Pta Δ*hopAZ1*(phopAZ1 1-200)	Isolate 6605 ΔRS0124775 carrying pDSK519-*hopAZ1* promoter::*hopAZ1*$^{1\text{-}200}$, Nal^r, Km^r	This study
Pta Δ*hopAZ1*(phopAZ1-3×HA)	Isolate 6605 ΔRS0124775 carrying pDSK519-*hopAZ1* promoter::*hopAZ1*-3×HA, Nal^r, Km^r	This study
Plasmids		
pHSG396	a pUC type of cloning vector, Cm^r	Takara
pK18*mobsacB*	Small mobilizable vector, sucrose sensitive (*sacB*); Km^r	Schäfer et al. (1994)
pK18*mobsac*BN	*Not*I site inserted between *Pst*I and *Hin*dIII site of MCS in pK18; Km^r	This study
Pta Δ*hrcC*	ΔRS0106115 fragment-containing pK18, Km^r	This study
Pta Δ*avrE1*	Isolate 6605 ΔRS0100760, Nal^r	This study
Pta Δ*avrPto4*	Isolate 6605, Δ*avrPto4*, Nal^r	This study
Pta Δ*hopAB3*	Isolate 6605 ΔRS0105230, Nal^r	This study
Pta Δ*hopAE1*	Isolate 6605 ΔRS0125645, Nal^r	This study
Pta Δ*hopAG1*Δ*hopAH1*Δ*hopAI1*	Isolate 6605 ΔRS0109770, ΔRS0109780, ΔRS0109785, Nal^r	This study
Pta Δ*hopAH2*	Isolate 6605 ΔRS0116920, Nal^r	This study
Pta Δ*hopAR1*	Isolate 6605, Δ*hopAR1*, Nal^r	This study
Pta Δ*hopAZ1*	Isolate 6605, ΔRS0114820, Nal^r	This study

TABLE 1 (Continued)

Bacterial strain/plasmid	Relevant characteristics	Reference or source
Pta Δ*hopBD1*	Isolate 6605, ΔRS0124775, Nal^r	This study
Pta Δ*hopE1*	Isolate 6605, Δ*hopBD1*, Nal^r	This study
Pta Δ*hopF2*	Isolate 6605, ΔRS0112920, Nal^r	This study
Pta Δ*hopI1*	Isolate 6605, ΔRS0109130, Nal^r	This study
Pta Δ*hopM1*Δ*avrF*	Isolate 6605, ΔRS0100770, Nal^r	This study
Pta Δ*hopO1-1*Δ*hopT1-1*	Isolate 6605, ΔRS01135, ΔRS01130, Nal^r	This study
Pta Δ*hopR1*	Isolate 6605, Δ*hopR1*, Nal^r	This study
Pta Δ*hopV1*	Isolate 6605, Δ*hopV1*, Nal^r	This study
Pta Δ*hopW1*	Isolate 6605, ΔRS0116415, Nal^r	This study
Pta Δ*hopX1*	Isolate 6605, ΔRS0121235, Nal^r	This study
pDSK519	Broad-host-range cloning vector; Km^r	Keen et al. (1988)
p*hopAZ1*	pDSK519 possessing expressible *hopAZ1*; Km^r	This study
p*hopAZ1*$^{1\text{-}100}$	pDSK519 possessing expressible *hopAZ1*$^{1\text{-}100}$; Km^r	This study
p*hopAZ1*$^{1\text{-}200}$	pDSK519 possessing expressible *hopAZ1*$^{1\text{-}200}$; Km^r	This study
p*hopAZ1*-3×HA	pDSK519 possessing expressible *hopAZ1*-3×HA; Km^r	This study
pBCKH 35S::*gfp*	pBCKH binary vector possessing expressible GFP, Km^r, Hyg^r	Mitsuda et al. (2006)
pGWB5	Gateway cloning binary vector, Km^r, Hyg^r	Nakagawa et al. (2007)
pGWB5 35S::*hopAZ1-gfp*	pGWB5 possessing expressible *hopAZ1-gfp*, Km^r, Hyg^r	This study
pGWB5 35S::*hopAZ1*$^{1\text{-}100}$*-gfp*	pGWB5 possessing expressible *hopAZ1*$^{1\text{-}100}$*-gfp*, Km^r, Hyg^r	This study
pGWB5 35S::*hopAZ1*$^{1\text{-}200}$*-gfp*	pGWB5 possessing expressible *hopAZ1*$^{1\text{-}200}$*-gfp*, Km^r, Hyg^r	This study

Note: Seven-digit annotation and five-digit annotation indicate the database source for Pta 6605 and Pta 11528, respectively. The effector gene names listed are not annotated in the database.

Amp^r, ampicillin resistant; Cm^r, chloramphenicol resistant; Hyg^r, hygromycin resistant; Km^r, kanamycin resistant, Nal^r, nalidixic acid resistant.

(Psv) NCPPB 3335 has been reported to suppress callose deposition and ROS production (Matas et al., 2014). The HopAZ1$_{Psv3335}$ sequence is highly conserved and has 96% sequence homology to HopAZ1$_{Pta6605}$; however, HopAZ1$_{Psv3335}$ lacks approximately 95 amino acids of the C-terminal sequence compared to the HopAZ1 sequences of other *Pseudomonas* strains (Figure 4a). To investigate the site of HopAZ1 required for N509 to induce an HR, we constructed a HopAZ1 construct with a C-terminal stepwise truncation and introduced the Pta 6605 Δ*hopAZ1* mutant to test its ability to induce an HR. Infiltration inoculation results showed that both Pta 6605 Δ*hopAZ1* (p*hopAZ1* 1–100) and Pta 6605 Δ*hopAZ1* (p*hopAZ1* 1–200) strains did not lead to an HR in N509 (Figure 4b). These results imply that the entire length of HopAZ1$_{Pta6605}$ is required to induce an HR in N509.

Because the deletion of 59 amino acids in the C-terminal region of HopAZ1 resulted in a loss of HR-inducing ability, we investigated the effect of tagging HopAZ1 with a C-terminal green fluorescent protein (GFP) tag on its HR-inducing ability (Figure 4c). Our results showed that adding a GFP-tag to the C-terminal region of HopAZ1 did not affect its ability to induce an HR in N509. We confirmed the stability of truncated HopAZ1 proteins by immunoblotting. Full-length HopAZ1-GFP and truncated HopAZ1-GFP proteins were detected in Shiroensyu, whereas full-length HopAZ1-GFP protein could not be detected in N509 (Figure S6).

Next, we analysed the subcellular localization of functional HopAZ1-GFP by a transient expression system using *N. benthamiana*. Confocal microscopy revealed that HopAZ1-GFP localized to the nucleus, cytoplasm, and plasma membrane (Figure 4d). We confirmed the subcellular localization of HopAZ1-GFP by subcellular fractionation. HopAZ1-GFP was detected in the microsomal fraction, suggesting that HopAZ1 may target proteins associated with microsome-related proteins (Figure S7).

In this study, we found that *N. tabacum* 'N509' exhibited disease resistance dependent on the presence of the T3E HopAZ1. As mentioned above, N509 was derived from a cross between Shiroensyu and Burley 21, which carries Pta-resistance derived from *N. longiflora*. *N. longiflora* is a wild tobacco species from South America that was reported to be resistant to Pta strain 11528 and has a history of being used as a genetic resource for resistance to several other important diseases (Knoche et al., 1987; Schweppenhauser, 1975; Valleau et al., 1960). Because Pta strains 6605 and 11528 both possess *hopAZ1* in their genomes, we assumed that Burley 21, N509, and *N. longiflora* have a common *R* gene that recognizes HopAZ1. Interestingly, an HR was not strongly induced in *N. longiflora* by the Pta 6605 inoculation test (Figures S4 and S5). Although the detailed molecular mechanism is unknown, *N. longiflora* seems to have a complex molecular mechanism of resistance to Pta.

Screening using a series of Pta T3E deletion mutants revealed that resistant N509 recognizes HopAZ1$_{Pta6605}$ (Figures 2 and 3). HopAZ1 is conserved in at least 12 of the 29 *Pseudomonas* strains whose genomes have been sequenced (Laflamme et al., 2020).

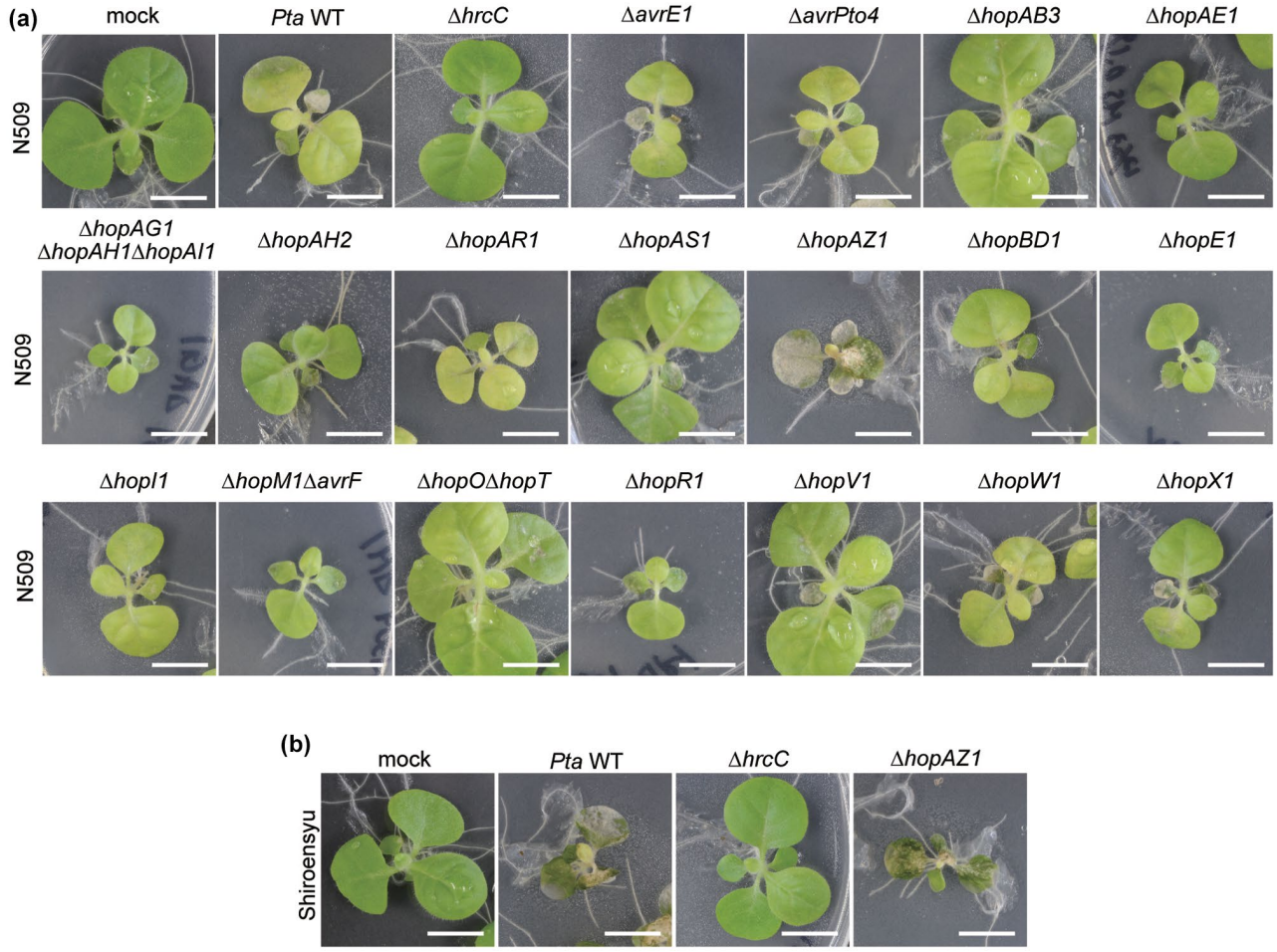

FIGURE 2 Identification of avirulent type III effectors recognized by *Nicotiana tabacum* 'N509'. (a) A flood inoculation test of *Pseudomonas amygdali* pv. *tabaci* (Pta) wild type (WT) and Pta type III effector (T3E) deletion strains with the Pta-resistant cultivar N509. The concentration of the inoculum was adjusted to an OD_{600} = 0.002. The photograph shows representative N509 plants 5 days postinoculation (dpi). The hypersensitive response (HR) assays were repeated at least twice with three independent plants with similar results. The scale bar represents 1 cm. (b) A flood inoculation test of Pta WT and Pta T3E deletion strains with the Pta-susceptible cultivar Shiroensyu. The concentration of the inoculum was adjusted to an OD_{600} = 0.002. The photograph shows representative Shiroensyu plants 5 dpi. Inoculation tests were repeated at least twice with three independent plants with similar results. The scale bar represents 1 cm

Comparative genome analysis has proposed the possibility that HopAZ1 is a candidate determinant of host specificity for *Corylus avellana* (hazelnut) in *P. syringae* pv. *avellanae*, a causative agent of decline disease in hazelnut (O'Brien et al., 2012). $HopAZ1_{Psv3335}$ consists of 122 amino acids lacking the C-terminal end of the HopAZ1 encoded by other *P. syringae* pathovars (Figure 4a; Matas et al., 2014). In addition to inhibiting the PTI response, $HopAZ1_{Psv3335}$ has also been reported to inhibit ETI-like cell death (Matas et al., 2014). Because $HopAZ1_{Pta6605}$ lacking the C-terminus does not induce an HR in N509 (Figures 4b and S6), the loss of $HopAZ1_{Psv3335}$ may have been to avoid recognition by host defence mechanisms. The function of the HopAZ1 protein as an effector, however, is still undefined and the host factors targeted by HopAZ1 are also unknown. Future work will be required to identify the host targets of $HopAZ1_{Pta6605}$.

We also tested the role of HopAZ1 as a virulence factor using the susceptible cv. Shiroensyu; however, there was no apparent difference in the size of bacterial populations or in disease symptoms between Pta 6605 and the Pta 6605 Δ*hopAZ1* mutant (Figure 3b). It is difficult to determine the importance of HopAZ1 in the virulence of Pta 6605 using a single deletion mutation in *hopAZ1*. The construction of multiple mutants, such as *P. syringae* pv. *tomato* DC3000 D28E (Cunnac et al., 2011), and the reintroduction of effectors into these mutants (Wei et al., 2018), might lead to an improved understanding of their importance for virulence.

$HopAZ1_{Pta6605}$-GFP mainly localized to the microsomal fraction when transiently expressed in *N. benthamiana* leaves (Figures 4d and S7). A previous report demonstrated that HopAZ1 of *P. syringae* pv. *actinidiae* (Pac) localizes to the cytoskeleton (Choi et al., 2017). Because the N-terminal sequence of $HopAZ1_{Pac}$ is shorter (219 amino acids) than that of $HopAZ1_{Pta6605}$, it is possible that the N-terminal sequence of HopAZ1 is responsible for the different subcellular localization patterns.

In summary, we demonstrated that $HopAZ1_{Pta6605}$ is a T3E recognized by Pta-resistant tobacco cvs Burley 21 and N509. The next

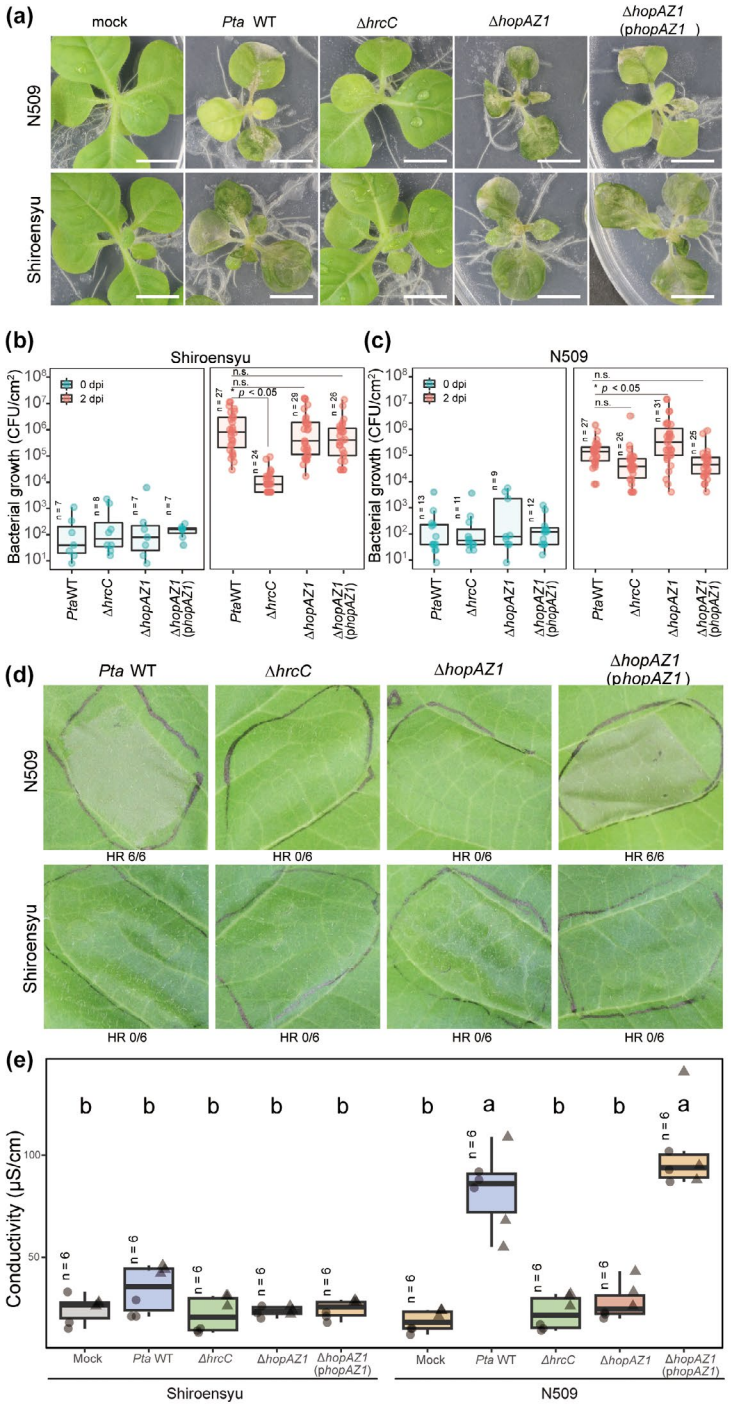

FIGURE 3 HopAZ1 induced a hypersensitive response (HR) in *Nicotiana tabacum* 'N509'. (a) Flood inoculation test of *Pseudomonas amygdali* pv. *tabaci* (Pta) Δ*hopAZ1* and Pta Δ*hopAZ1* (p*hopAZ1*) in the resistant cultivar N509 and the susceptible cultivar Shiroensyu. Two-week-old plants were flood-inoculated with each strain (OD_{600} = 0.002) and photographed 4 days postinoculation (dpi). Inoculation tests were repeated at least twice with three independent plants with similar results. (b, c) Bacterial populations in Shiroensyu and N509 leaves at 0 and 2 dpi. The five times results were combined and illustrated in a box plot. Boxes show upper and lower quartiles of the data, and black lines represent the medians. Each dot represents raw data. The numbers of the graph indicate the total number of individuals used in the experiment. Statistical tests were performed using the Dunnett test (*$p < 0.05$). (d) Photographs of HR induction in Pta-infiltrated plants. Eight-week-old plants were infiltrated with Pta wild type (WT), Pta Δ*hrcC*, Pta Δ*hopAZ1*, or Pta Δ*hopAZ1* (p*hopAZ1*), whose concentrations were adjusted to an OD_{600} = 0.02 and photographed at 24 h postinoculation (hpi). The HR assays were repeated three times with three independent plants with similar results (the total number of biological replicates; $n = 9$). (e) Measurement of ion leakage after Pta infiltration. The concentration of each Pta strain was adjusted to an OD_{600} = 0.02. Leaves were inoculated by infiltration. Leaf discs were prepared from the inoculation area, floated in deionized water and measured for ion leakage 24 hpi. The two times results were combined and displayed in this boxplot. Boxes show upper and lower quartiles of the data, and black lines represent the medians. Each dot represents the raw data. Statistically significant differences are indicated by different letters ($p < 0.01$, Tukey HSD test)

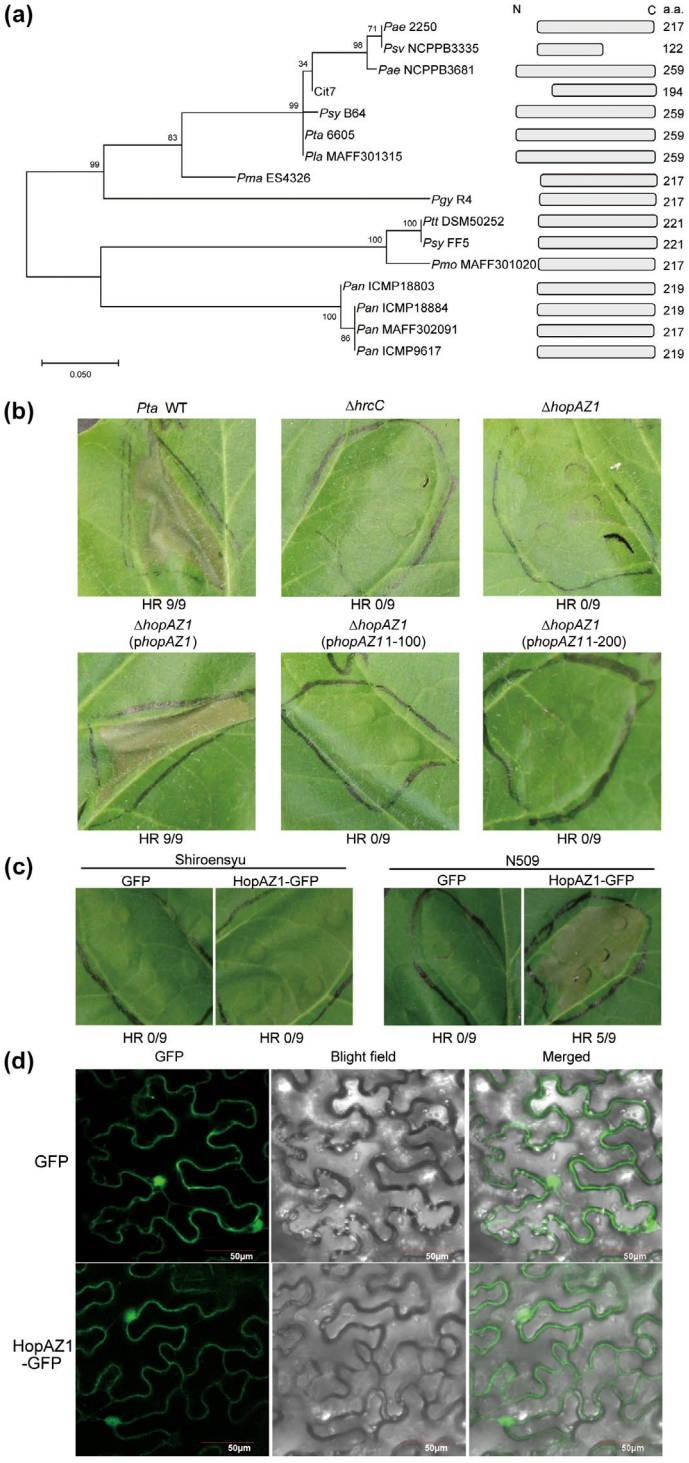

FIGURE 4 Structure of HopAZ1 and its HR-induction activity. (a) A phylogenetic tree based on the deduced amino acid sequences of HopAZ1 (left) and the primary structure of HopAZ1 (right). Numbers at the nodes are bootstrap values as percentages. The scale bar indicates the units of the number of amino acid substitutions per site. Each box indicates the HopAZ1 structure, and the numbers on the right indicate the number of amino acids in each deduced HopAZ1 sequence. (b) Effect of C-terminal deletions of HopAZ1 on hypersensitive response (HR) induction in N509. Eight-week-old cv. N509 plants were infiltrated with each strain (OD_{600} = 0.02). An HR was observed at 48 h postinoculation (hpi). The infiltration assays were repeated three times with three independent plants with similar results. The numbers below the photographs indicate the number of HR-induced individuals compared with the total number of examined plants. (c) HR in tobacco cv. N509 induced by agroinfiltration. A needleless syringe was used to infiltrate an *Agrobacterium* solution (OD_{600} = 0.3) on cvs Shiroensyu and N509. An HR was observed at 48 hpi. Agroinfiltration assays were repeated three times with three independent plants with similar results. The numbers below each photograph indicate the number of HR-induced individuals compared with the total number of examined plants. (d) Subcellular localization of HopAZ1-GFP in *Nicotiana benthamiana*. The scale bar represents 50 μm

challenge will be to find resistance genes that recognize HopAZ1, a challenging task given the size of the tobacco genome. Recent studies have established that a genome-wide *R* gene search method using a hairpin-RNAi library was suitable for isolating resistance genes in *N. benthamiana* (Brendolise et al., 2017). The resistance gene *Rpa1* (*Resistance to P. syringae pv. actinidiae* 1) was also isolated using this experimental method in *N. tabacum* (Yoon & Rikkerink, 2020). As more genome sequence information for *N. tabacum* is becoming available (Sierro et al., 2014), we hope to use these technologies to decipher the HopAZ1 recognition mechanism of *N. tabacum* 'N509' in the future.

ACKNOWLEDGEMENTS

The authors thank the Leaf Tobacco Research Laboratory of Japan Tobacco Inc. for providing Pta 6605, tobacco cultivars, and wild tobacco plants. We also thank the National BioResource Project (NIG, Japan): *Escherichia coli* for providing *E. coli* S17-1. This work was supported in part by a Grants-in-Aid for Scientific Research

(19H02956) from the Ministry of Education, Culture, Sports, Science and Technology of Japan.

CONFLICTS OF INTEREST

The authors declare that they have no conflicts of interest.

DATA AVAILABILITY STATEMENT

The data that support the findings of this study are available from the corresponding author upon reasonable request. As tobacco seeds are not transferable from us, please contact the Leaf Tobacco Research Laboratory of Japan Tobacco Inc.

ORCID

Yoshiteru Noutoshi https://orcid.org/0000-0001-8140-3722
Yuki Ichinose https://orcid.org/0000-0002-7767-7912
Hidenori Matsui https://orcid.org/0000-0003-3386-7180

REFERENCES

Ayliffe, M.A. (2004) Molecular genetics of disease resistance in cereals. *Annals of Botany*, 94, 765–773.

Baltrus, D.A., Nishimura, M.T., Romanchuk, A., Chang, J.H., Mukhtar, M.S., Cherkis, K. et al. (2011) Dynamic evolution of pathogenicity revealed by sequencing and comparative genomics of 19 *Pseudomonas syringae* isolates. *PLoS Pathogens*, 7, e1002132.

Block, A. & Alfano, J.R. (2011) Plant targets for *Pseudomonas syringae* type III effectors: virulence targets or guarded decoys? *Current Opinion in Microbiology*, 14, 39–46.

Brendolise, C., Montefiori, M., Dinis, R., Peeters, N., Storey, R.D. & Rikkerink, E.H. (2017) A novel hairpin library-based approach to identify NBS–LRR genes required for effector-triggered hypersensitive response in *Nicotiana benthamiana*. *Plant Methods*, 13, 32.

Choi, S., Jayaraman, J., Segonzac, C., Park, H.-J., Park, H., Han, S.-W. et al. (2017) *Pseudomonas syringae* pv. *actinidiae* type III effectors localized at multiple cellular compartments activate or suppress innate immune responses in *Nicotiana benthamiana*. *Frontiers in Plant Science*, 8, 2157.

Cunnac, S., Chakravarthy, S., Kvitko, B.H., Russell, A.B., Martin, G.B. & Collmer, A. (2011) Genetic disassembly and combinatorial reassembly identify a minimal functional repertoire of type III effectors in *Pseudomonas syringae*. *Proceedings of the National Academy of Sciences of the United States of America*, 108, 2975–2980.

Dillon, M.M., Almeida, R.N.D., Laflamme, B., Martel, A., Weir, B.S., Desveaux, D. et al. (2019) Molecular evolution of *Pseudomonas syringae* type III secreted effector proteins. *Frontiers in Plant Science*, 10, 418.

Gimenez-Ibanez, S., Boter, M., Fernández-Barbero, G., Chini, A., Rathjen, J.P. & Solano, R. (2014) The bacterial effector HopX1 targets JAZ transcriptional repressors to activate jasmonate signaling and promote infection in *Arabidopsis*. *PLoS Biology*, 12, e1001792.

Gimenez-Ibanez, S., Hann, D.R., Chang, J.H., Segonzac, C., Boller, T. & Rathjen, J.P. (2018) Differential suppression of *Nicotiana benthamiana* innate immune responses by transiently expressed *Pseudomonas syringae* type III effectors. *Frontiers in Plant Science*, 9, 688.

Heggestad, H.E., Clayton, E.E., Neas, M.O. & Skoog, H.A. (1960) Development of Burley 21, the first wildfire-resistant tobacco variety, including results of variety trials. *Bulletins*. Available at: https://trace.tennessee.edu/utk_agbulletin/265 [Accessed 8 February 2022].

Holsters, M., Silva, B., Van Vliet,F., Genetello, C., De Block, M., Dhaese, P., Depicker, A., Inzé, D., Engler, G., Villarroel, R., Van Montagu, M. & Schell, J. (1980) The functional organization of the nopaline *A. tumefaciens* plasmid pTiC58. *Plasmid*, 3, 212–230.

Jones, J.D.G. & Dangl, J.L. (2006) The plant immune system. *Phytopathology*, 77, 1364–1368.

Keen, N.T., Tamaki, S., Kobayashi, D. & Trollinger, D. (1988) Improved broad-host-range plasmids for DNA cloning in Gram-negative bacteria. *Gene*, 70, 191–197.

Knoche, K.K., Clayton, M.K. & Fulton, R.W. (1987) Comparison of resistance in tobacco to *Pseudomonas syringae* pv. *tabaci* races 0 and 1 by infectivity titrations and bacterial multiplication. *Phytopathology*, 77, 1364–1368.

Kourelis, J. & van der Hoorn, R.A.L. (2018) Defended to the nines: 25 years of resistance gene cloning identifies nine mechanisms for R protein function. *The Plant Cell*, 30, 285–299.

Laflamme, B., Dillon, M.M., Martel, A., Almeida, R.N.D., Desveaux, D. & Guttman, D.S. (2020) The pan-genome effector-triggered immunity landscape of a host–pathogen interaction. *Science*, 367, 763–768.

Marutani, M., Taguchi, F., Shimizu, R., Inagaki, Y., Toyoda, K., Shiraishi, T. et al. (2005) Flagellin from *Pseudomonas syringae* pv. *tabaci* induced *hrp*-independent HR in tomato. *Journal of General Plant Pathology*, 71, 289–295.

Matas, I.M., Castañeda-Ojeda, M.P., Aragón, I.M., Antúnez-Lamas, M., Murillo, J., Rodríguez-Palenzuela, P. et al. (2014) Translocation and functional analysis of *Pseudomonas savastanoi* pv. *savastanoi* NCPPB 3335 type III secretion system effectors reveals two novel effector families of the *Pseudomonas syringae* complex. *Molecular Plant-Microbe Interactions*, 27, 424–436.

Matsui, H., Nishimura, T., Asai, S., Masuda, S., Shirasu, K., Yamamoto, M. et al. (2021) Complete genome sequence of *Pseudomonas amygdali* pv. *tabaci* strain 6605, a causal agent of tobacco wildfire disease. *Microbiology Resource Announcements*, 10, e00405-21.

Mitsuda, N., Hiratsu, K., Todaka, D., Nakashima, K., Yamaguchi-Shinozaki, K. & Ohme-Takagi, M. (2006) Efficient production of male and female sterile plants by expression of a chimeric repressor in *Arabidopsis* and rice. *Plant Biotechnology Journal*, 4, 325–332.

Nakagawa, T., Kurose, T., Hino, T., Tanaka, K., Kawamukai, M., Niwa, Y. et al. (2007) Development of series of Gateway binary vectors, pGWBs, for realizing efficient construction of fusion genes for plant transformation. *Journal of Bioscience and Bioengineering*, 104, 34–41.

O'Brien, H.E., Thakur, S., Gong, Y., Fung, P., Zhang, J., Yuan, L. et al. (2012) Extensive remodeling of the *Pseudomonas syringae* pv. *avellanae* type III secretome associated with two independent host shifts onto hazelnut. *BMC Microbiology*, 12, 141.

Schäfer, A., Tauch, A., Jäger, W., Kalinowski, J., Thierbachb, G. & Pühler, A. (1994) Small mobilizable multi-purpose cloning vectors derived from the *Escherichia coli* plasmids pK18 and pK19: selection of defined deletions in the chromosome of *Corynebacterium glutumicum*. *Gene*, 145, 69–73.

Schweppenhauser, M.A. (1975) Rootknot resistance from *Nicotiana longiflora*. *Tobacco Science*, 19–10, 26–29.

Shimizu, R., Taguchi, F., Marutani, M., Mukaihara, T., Inagaki, Y., Toyoda, K. et al. (2003) The Δ*fliD* mutant of *Pseudomonas syringae* pv. *tabaci*, which secretes flagellin monomers, induces a strong hypersensitive reaction (HR) in non-host tomato cells. *Molecular Genetics and Genomics*, 269, 21–30.

Sierro, N., Battey, J.N.D., Ouadi, S., Bakaher, N., Bovet, L., Willig, A. et al. (2014) The tobacco genome sequence and its comparison with those of tomato and potato. *Nature Communications*, 5, 3833.

Studholme, D.J. (2011) Application of high-throughput genome sequencing to intrapathovar variation in *Pseudomonas syringae*: *Pseudomonas syringae* genomics. *Molecular Plant Pathology*, 12, 829–838.

Valleau, W.D., Stokes, G.W. & Johnson, E.M. (1960) Nine years' experience with the *Nicotiana longiflora* factor for resistance to *Phytophthora parasitica* var. *nicotianae* in the control of black shank. *Tobacco Science*, 4–19, 92–94.

Wei, H.-L., Zhang, W. & Collmer, A. (2018) Modular study of the type III effector repertoire in *Pseudomonas syringae* pv. *tomato* DC3000 reveals a matrix of effector interplay in pathogenesis. *Cell Reports*, 23, 1630–1638.

Winsor, G.L., Griffiths, E.J., Lo, R., Dhillon, B.K., Shay, J.A. & Brinkman, F.S.L. (2016) Enhanced annotations and features for comparing thousands of *Pseudomonas* genomes in the Pseudomonas genome database. *Nucleic Acids Research*, 44, D646–D653.

Xin, X.-F., Kvitko, B. & He, S.Y. (2018) *Pseudomonas syringae*: what it takes to be a pathogen. *Nature Reviews Microbiology*, 16, 316–328.

Yoon, M. & Rikkerink, E.H.A. (2020) *Rpa1* mediates an immune response to *avrRpm1*$_{Psa}$ and confers resistance against *Pseudomonas syringae* pv. *actinidiae*. *The Plant Journal*, 102, 688–702.

Yuan, M., Ngou, B.P.M., Ding, P. & Xin, X.-F. (2021) PTI–ETI crosstalk: an integrative view of plant immunity. *Current Opinion in Plant Biology*, 62, 1369–5266.

SUPPORTING INFORMATION

Additional supporting information may be found in the online version of the article at the publisher's website.

How to cite this article: Kashihara, S., Nishimura, T., Noutoshi, Y., Yamamoto, M., Toyoda, K., Ichinose, Y. & et al (2022) HopAZ1, a type III effector of *Pseudomonas amygdali* pv. *tabaci*, induces a hypersensitive response in tobacco wildfire-resistant *Nicotiana tabacum* 'N509'. *Molecular Plant Pathology*, 00, 1–10. https://doi.org/10.1111/mpp.13198